

Electronic Supplementary Information (ESI) for
Copper aryl nitrene formation by oxidation of arylamine with copper(II)oxyl

Noël R.M. de Kler^a and Jana Roithová*^a

^a Department of Spectroscopy and Catalysis, Institute for Molecules and Materials, Radboud University, Heyendaalseweg 135 6525 AJ Nijmegen (The Netherlands) E-mail: J.Roithova@science.ru.nl

Content

Experimental details	3
Generation of $[\text{Cu}(\text{L})\text{ClO}_3]^+$ complexes	5
IRPD spectrum (7b, m/z 366)	7
Kinetic isotope effect (7b, m/z 366).....	8
Gas phase reactivity (7b, m/z 366)	13
IRPD and reactivity of $[\text{Cu}(\text{TPA-OH})]^+$	15
Potential energy surfaces	16

Experimental details

Mass spectrometry

The experiments were performed with a triple-quadrupole instrument TSQ 7000 (Finnigan) equipped with an electrospray ionization (ESI) source. Solutions were introduced into the instrument by a fused-silica capillary in solution with a slight overpressure. The TSQ has a quadrupole–octopole–quadrupole geometry that allows MS and MS/MS experiments (collision-induced dissociation experiments and reactivity studies). For the MS/MS experiments, the reactant ions were mass selected by the first quadrupole and were guided through the octopole collision cell. The pressure of the gas in the collision cell was measured by a baratron. The collision energy was set by the potential offset between the octopole and the ion source. The offset corresponding to zero collision energy was determined by retarding potential analysis. The reactant as well as the product ions were mass analyzed by the second quadrupole.

Collision energy expressed in energy center of mass frame and calculated via the formula: $E_{cm} = E_{lab} \cdot m / (m + M)$. Where E_{lab} is the experimental energy in eV, m is the mass of the neutral collision gas (Xenon, 131.29) and M is the mass of the ion.

Generation of $[(\text{CuTPA}-(\text{NH}_2)_{0-2})(\text{ClO}_3)]^+$ (**1a-1c**)

The TPA ligand (**a**) was bought from Sigma-Aldrich. All other chemicals were commercially available.

A solution of the ligand (6 μL , 8.1 mM, in MeOH) was mixed with a $[\text{Cu}(\text{ClO}_3)_2]^+$ solution (2 μL , 0.17 M, in MeOH) and diluted to 3 mL with MeOH to yield a final concentration of the ligand (0.02 mM) and $[\text{Cu}(\text{ClO}_3)_2]^+$ (0.11 mM).

Copper(II) chlorate (0.17 M stock solution) was prepared by addition of KClO_4 (292 mg, 2.12 mmol) to a solution of $\text{Cu}(\text{ClO}_4)_2 \cdot 6\text{H}_2\text{O}$ (292 mg, 0.79 mmol) in H_2O /methanol (0.17 M) and filtering out precipitated KClO_4 .

ESI parameters for the generation of **7b** (m/z 366): spray voltage 5kV, sheath gas pressure 5 psi, no auxiliary gas, capillary voltage 5, capillary temperature 200 °C and tube lens 90V. (Figure S1)

Generation of $[\text{Au}(\text{PMe}_3)]^+$

0.56 ml of a AgPF_6 solution in methanol (36.8 mM) was mixed with 1.5 mL $[\text{Au}(\text{Cl})(\text{PMe}_3)]^+$ in THF:MeOH (1:2)(13.8 mM) \rightarrow sonicate 20 min, filter with syringe filter. The $[\text{Au}(\text{PF}_6)(\text{PMe}_3)]$ solution (13.8 mM) was diluted 100x in MeOH (0.14 mM). ESI of the solution resulted in the generation of $[\text{AuPMe}_3]^+$ (m/z 273) (Figure S4).

Helium tagging IRPD

The instrument ISORI was used.^{2,3} The ions were generated via a TSQ Finnegan ESI source, mass-selected by the first quadrupole and transferred to the wire quadrupole ion trap by a quadrupole bender and an octopole. The trap operates at 2.3 K and the ions are trapped using helium buffer gas (pulsed in 4 pulses of 0.2 ms). The ions cool in the collisions with helium and finally form helium-tagged complexes that are further used to detect absorption of IR photons. Hence, the trapped ions were irradiated by a tunable IR OPO system. After irradiation, the ions were ejected from the trap and mass analyzed. Absorption of photons lead to vibrational excitation of the complexes, thereby causing the dissociation of the loosely bound helium atoms. The IRPD spectrum was thus obtained by monitoring of the number of helium

complexes as a function of the IR wavelength. The spectrum was plotted as the dissociation yield $1 - N_i / N_{i0}$, where N_i is the number of surviving complexes after laser irradiation (wavelength function) and N_{i0} is a reference complex count recorded by blocking the entrance of the IR light into the cold trap.

DFT calculations

The calculated structures were first optimized on a PM6 level and afterwards optimized with B3LYP functional and 6-31+G* basis set with D3 empirical correction (denoted as GD3BJ in the Gaussian program) for the PES of $\mathbf{1b}^+$ (Figure 2, Figure S8), as implemented in Gaussian 16 program.¹ For calculation of the reaction pathway of MeOH with ${}^3\mathbf{7b}^+$ the B3LYP-D3 functional was used with the 6-311+G(2d,p) basis set for the copper atom and the 6-31+G* basis for all remaining atoms. All reported structures are minima (no imaginary second derivative) or transition structures (one imaginary second derivative corresponding to the reaction coordinate) on the PES. Intrinsic reaction coordinate calculations were used to confirm the reaction coordinates for the obtained transition structures. The Mulliken population analysis was performed for the optimized structures with a density calculated at the B3LYP/6-311G(2d,p) level (single-point calculation).

Pressure dependent reactivity measurements

Deuterated methanol mixtures were prepared and connected to the inlet system for the collision cell. The pressure in the collision cell and relative peak intensity was monitored over time while the pressure was slowly increased from 0 to 0.3 mTorr over 30 minutes. Afterwards the pressure is slowly decreased back to 0 mTorr over 20 minutes. Online monitoring of the pressure and relative intensities was done with a software developed in our group for reactivity experiments.

Generation of $[\text{Cu}(\text{L})\text{ClO}_3]^+$ complexes

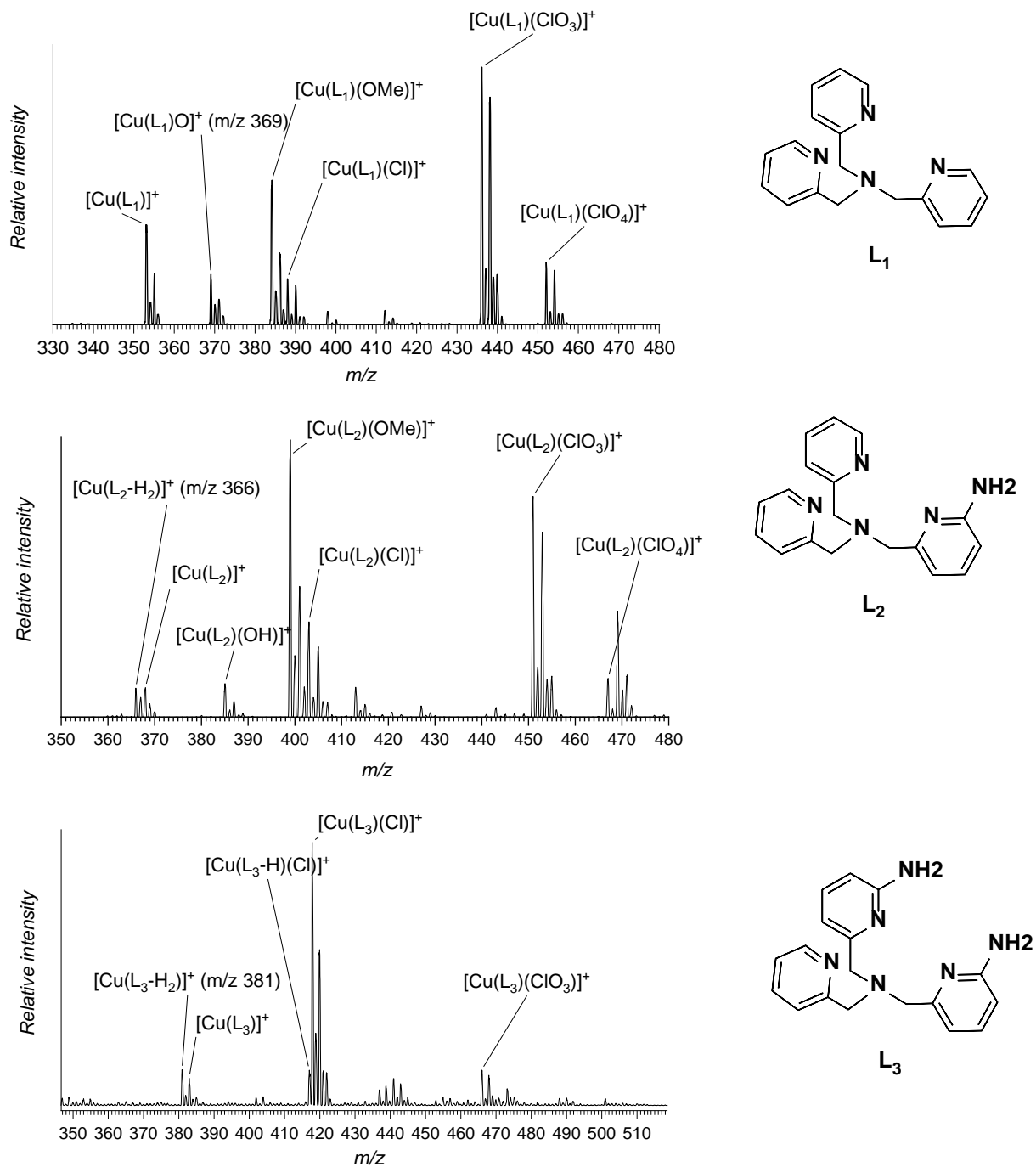
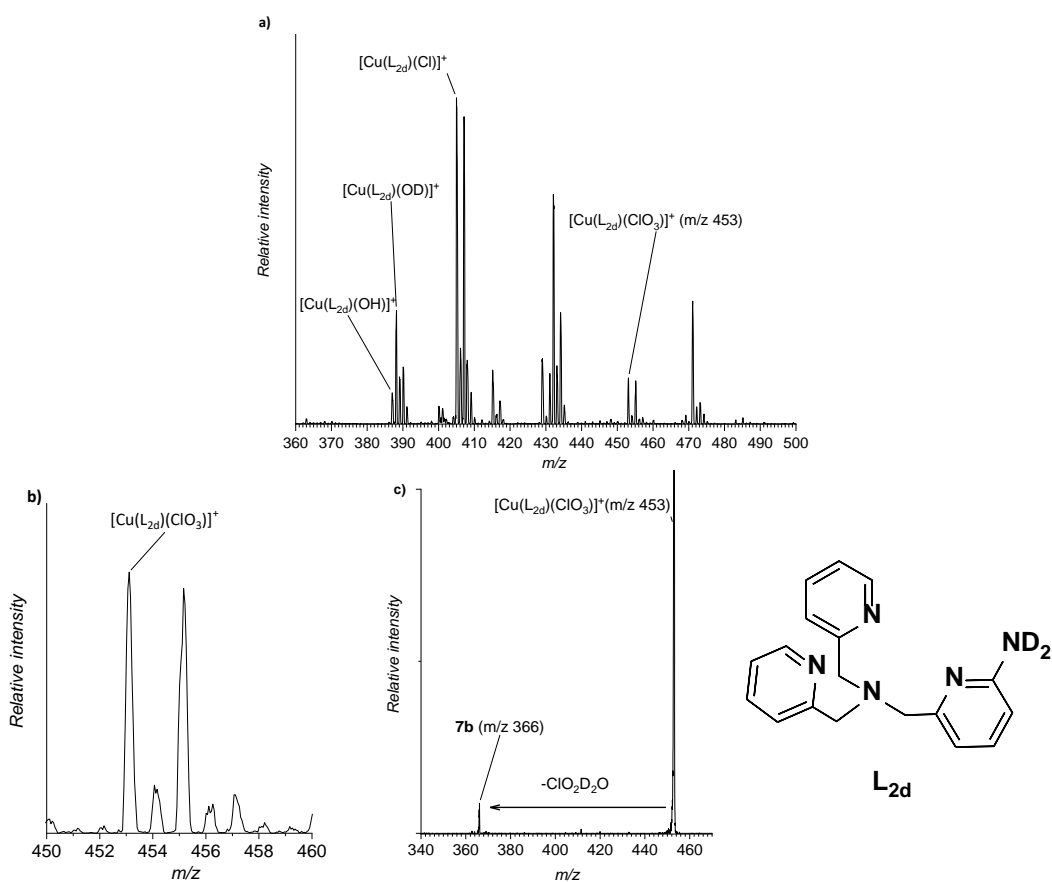


Figure S1. Electrospray ionization Q1 spectra of L₁ (top), L₂ (middle) and L₃ (bottom) mixed with $[\text{Cu}(\text{ClO}_3)_2]$ solutions. L₁=TPA, L₂=TPA^{NH2} and L₃=TPA^{(NH2)2}.

Deuterated complex $[\text{Cu}(\text{TPA}^{\text{ND}_2})(\text{ClO}_3)]^+$

The same procedure for the formation of $[\text{Cu}(\text{L})(\text{ClO}_3)]^+$ was used, but instead of diluting in MeOH the mixture was diluted in D_2O . The deuterated chlorate complex $[\text{Cu}(\text{TPA}^{\text{ND}_2})(\text{ClO}_3)]^+$ (m/z 453) was detected by electrospray ionization of this solution. The same CID pattern was observed for the non-deuterated complex, which means the oxidation process cannot be slowed enough in order to observe the $[\text{Cu}(\text{TPA}^{\text{ND}_2})(\text{O})]^+$ intermediate complex.



IRPD spectrum (7b, m/z 366)

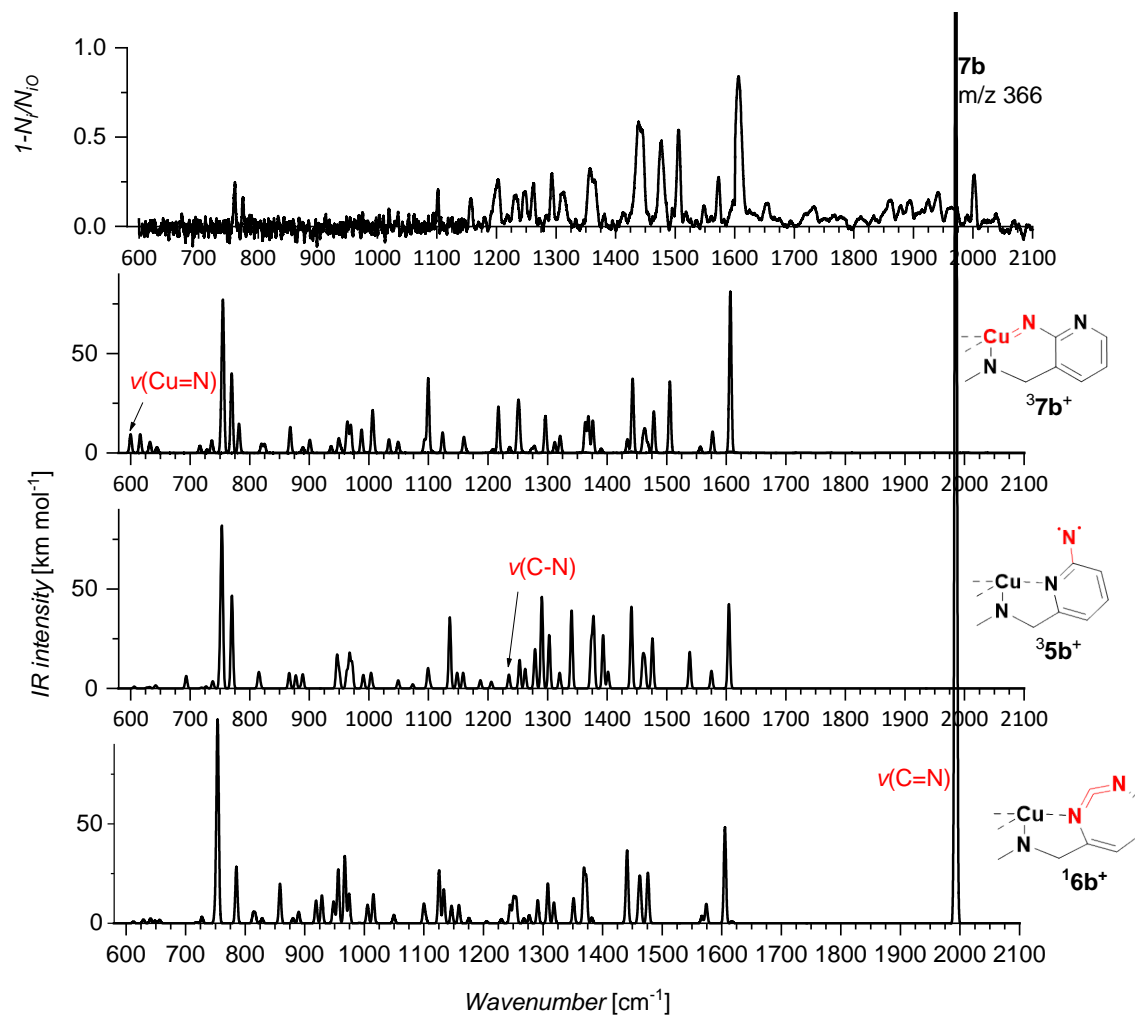


Figure S3. Helium tagging IRPD spectrum of $[\text{Cu}(\text{TPA-N})]^+$ (m/z 366) (top). The data was smoothed. The middle and bottom spectra are theoretically calculated (B3LYP/6-31+G*) and scaled by 0.97 factor to correct for anharmonicity.

Kinetic isotope effect (7b, m/z 366)

KIE MeOH from relative intensities

The relative concentrations of deuterated methanol's was determined via formation of adducts with $[\text{Au}(\text{PMe}_3)]^+$.

In order to have an exact ratio of gases in the collision cell, we have performed a reference reaction with $[\text{Au}(\text{PMe}_3)]^+$. Monoligated gold cations have a large affinity to bind a second ligand. In the presence of identical ligands differing only in isotopic labeling, the ratio of the gold adduct corresponds to the ratio of the labelled ligands in the collision cell.

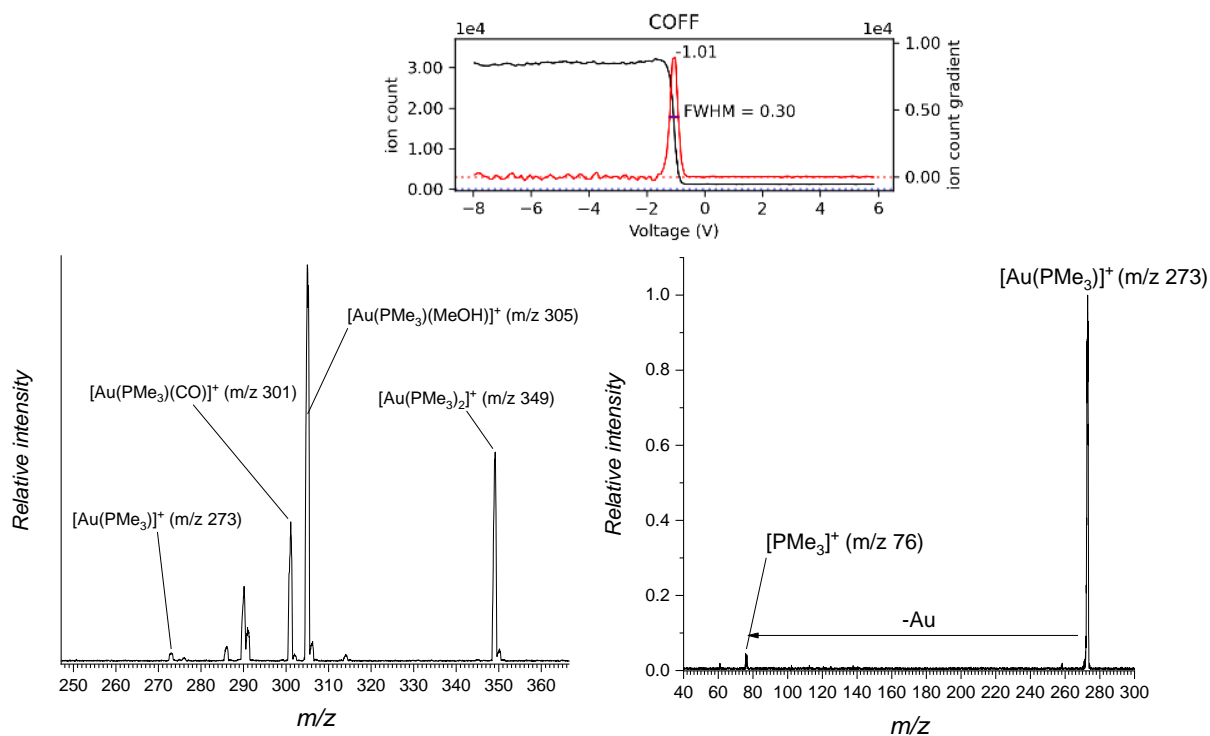


Figure S4. Kinetic energy distribution of $[\text{Au}(\text{PMe}_3)]^+$ and corresponding zero collision energy (top). Q1 source spectra of $[\text{Au}(\text{PMe}_3)(\text{PF}_6)]$ solution (left). CID of $[\text{Au}(\text{PMe}_3)]^+$ (m/z 273) at 0.1 mTorr Xenon and -6.2 eV collision energy (right).

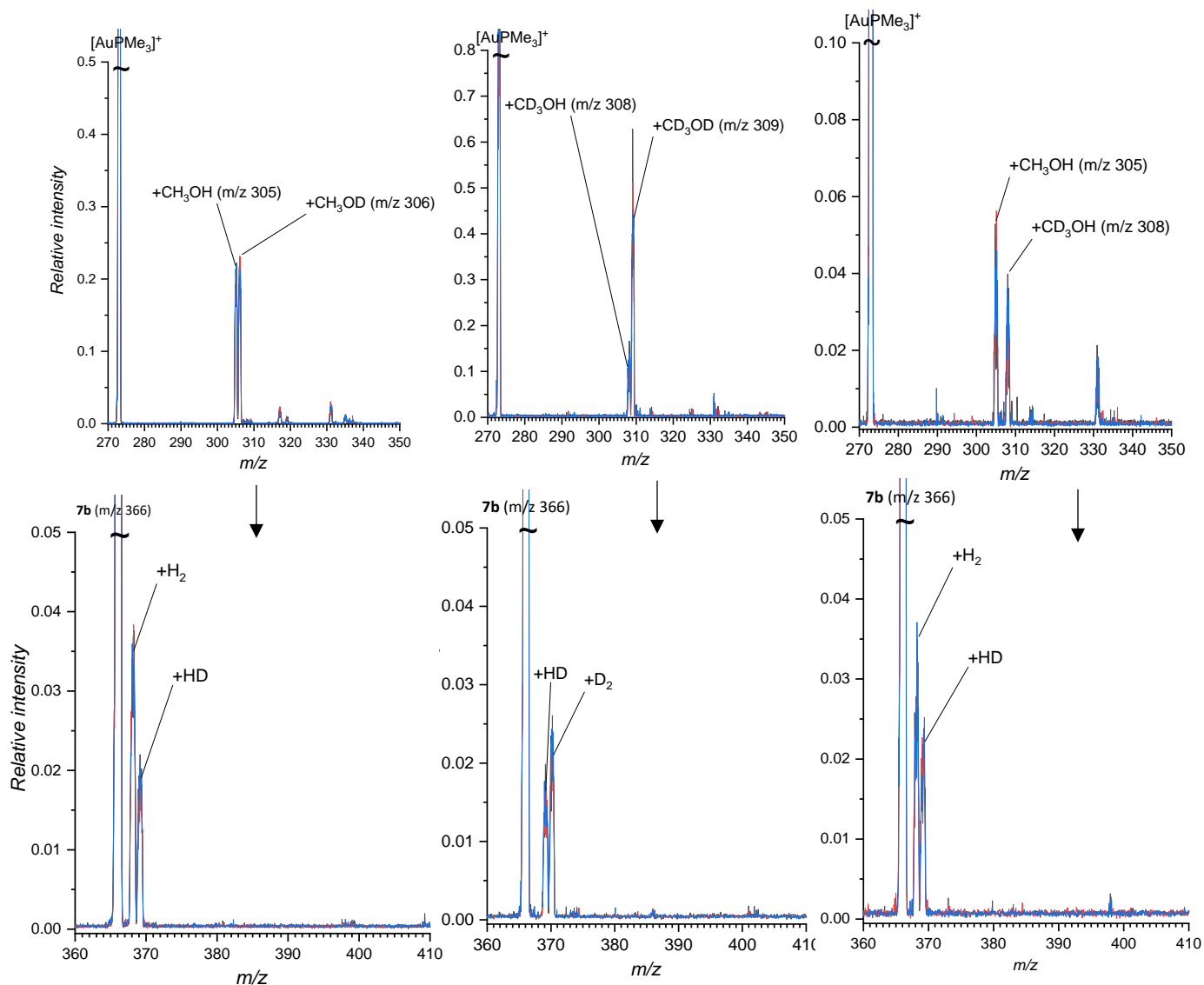


Figure S5. Determination of the relative concentration of labeled methanol's in the collision cell with $[\text{Au}(\text{PMe}_3)]^+$ (top spectra) from left to right: $\text{CH}_3\text{OH}/\text{CH}_3\text{OD}$ (left) $\text{CD}_3\text{OH}/\text{CH}_3\text{OH}$ (middle) and $\text{CD}_3\text{OH}/\text{CD}_3\text{OD}$ (right). Bottom spectra represent gas phase reactivity experiments of corresponding methanol mixture (0.15 mTorr) and $7b$ (m/z 366) at zero collision energy.

The figure below shows details for each measurement. The peaks were integrated with the origin integration tool. The *KIE* was calculated by dividing the peak area of the reaction channels (HD/H₂) or D₂/HD) by the relative concentration of methanol's determined with [AuPMe₃]⁺ (e.g. CH₃OD/CH₃OH). For each experiment three measurements were performed and the average with error bars are presented in the figure below. A *KIE* of ~2 was observed in these experiments.

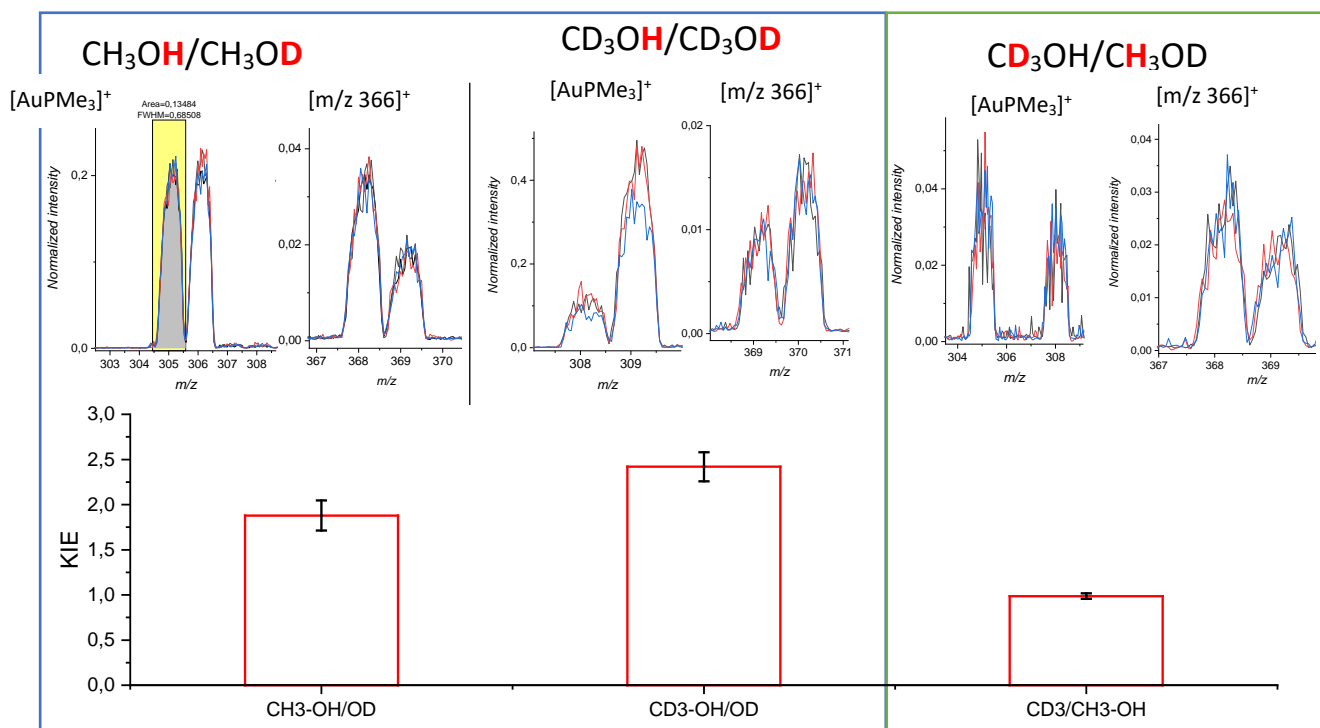


Figure S6. KIE based on relative intensity of reaction channel H₂/HD/D₂. Error bars represent the standard deviation of 3 measurements.

KIE MeOH from rate constant

First, the ratio between of the labelled methanol's was determined by the reaction with $[\text{Au}(\text{PMe}_3)]^+$ and was roughly 1:1 ratio. The reactivity was performed at nominally zero collision energy. Pressure of the substrate was slowly increased over a time period of 30 minutes from 0 to ~ 0.35 mTorr. Afterwards it was decreased back to 0 mTorr over a time period of 20 minutes. The measurements were recorded using software developed in our group by Jan Zelenka. The KIE effect was calculated ($\text{KIE} = k_{\text{H}_2}/k_{\text{HD}}$) where the reaction rate was extracted from the slope of the linear fit for each channel. KIE of CH/CD mixture was $0.219/0.234 = 0.93 \rightarrow \sim 1$. For OH/OD the KIE was $0.339/0.109 = 3.1$. Based on these results and the experiments with $[\text{AuPMe}_3]^+$ the KIE is approximately ~ 2.5 .

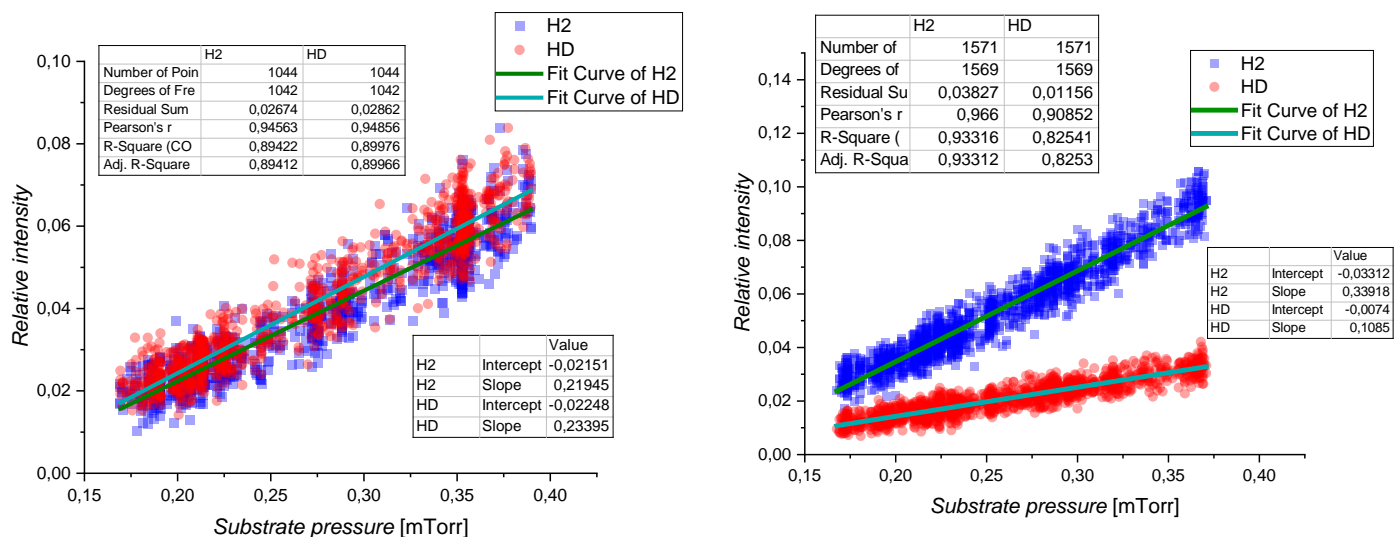
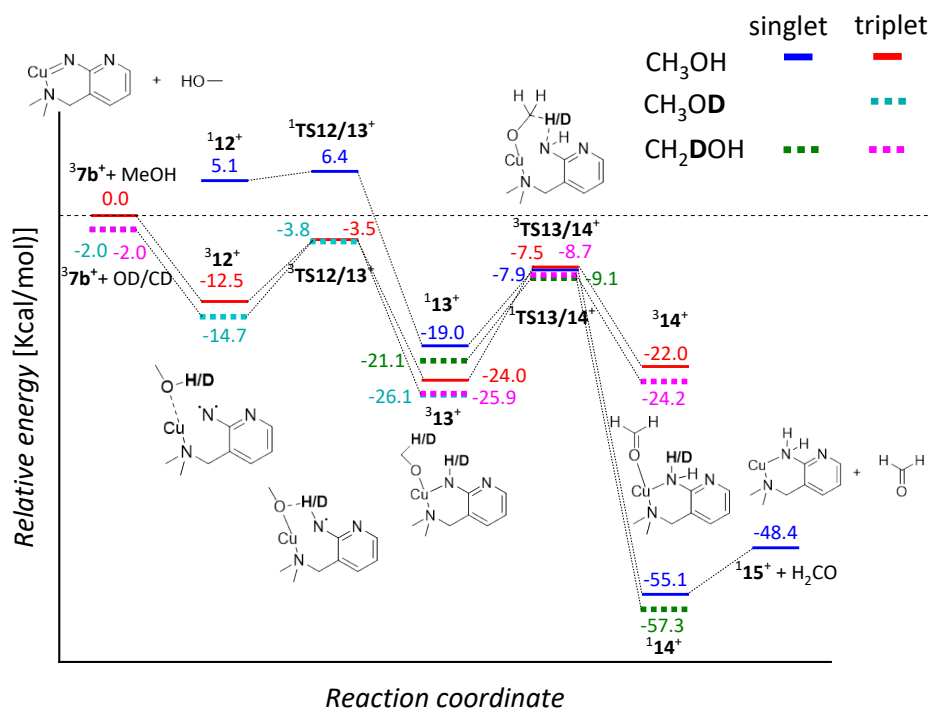


Figure S7. Pressure dependent reactivity measurements. The relative intensities of the reaction channels $+\text{H}_2$ and $+\text{HD}$ related to the parent ion are plotted versus the substrate concentration in the collision cell. The blue curves represent H_2 channel and red curves represent HD channels. Left graph: Mixture of $\text{CD}_3\text{OH}/\text{CH}_3\text{OH}$. Right graph: Mixture of $\text{CH}_3\text{OH}/\text{CH}_3\text{OD}$.

KIE MeOH theoretical

The potential energy surface of the reaction of **7b** with methanol was calculated in the Figure below. Modeling of the KIE was performed by single point calculations with CH₃OD and CH₂DOH (B3LYP-6-311+G(2d,p) on copper and B3LYP-6-31+G* on all other atoms). The KIE was calculated in the table below, for OH abstraction the KIE was calculated in the triplet state as 6.15.



	Energies (0K) in hartrees				ddG (Hartrees)	ddG (J/mol)	RT (J/mol)	KIE
	OH	OH	OD	CD				
	s	t	t	s	(dG _{OH} -dG _{OD})	*2625.5*1000		e ^(-ddG/RT)
7b+MeOH								
12		-2725.695779	-2725.699443					
TS12/13		-2725.681406	-2725.683355		-0.001715	-4502.7325	2478.8191	6.15
13	-2725.706040			-2725.709458				
TS13/14	-2725.688439			-2725.690383	-0.001474	-3869.986999	2478.8191	4.76
14				-2725.767216				

Figure S8. Potential energy surface the reaction of ³**7b**⁺ with deuterated methanol for calculation of the KIE (top). Calculated on B3LYP level with 6-31+G* basis set on light atoms and 6-311+G(2d,p) basis set on copper. The relative energies at 0K are presented in Kcal/mol. The table below represents the calculation of the KIE. The energies are given at 0K and are expressed in Hartrees.

KIE for 1,4CHD reaction

A KIE of ~ 2.5 was observed for HAT from 1,4-cyclohexadiene by **7b** (m/z 366). The KIE was calculated by dividing the maximum intensity of the C-H reaction channel by the maximum intensity of the C-D reaction channel (Figure S9, table S1).

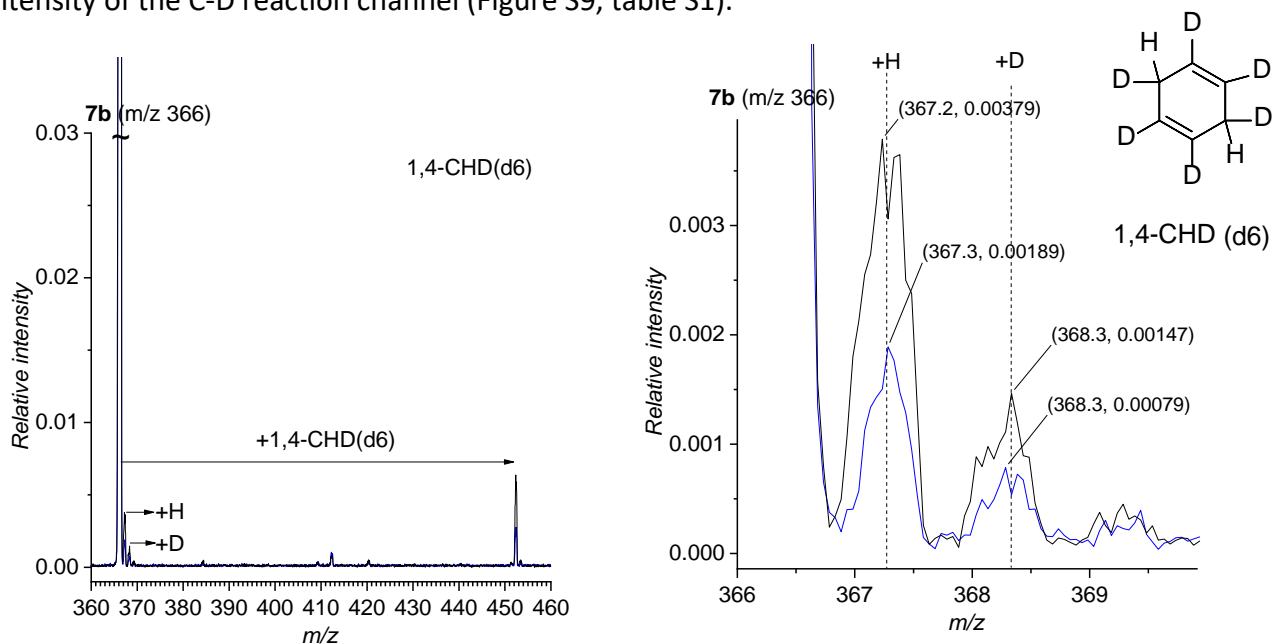


Figure S9. Left: Reactivity of **7b** (m/z 366) with 1,4-cyclohexadiene (d_6) at 0.3 (black) and 0.2 (blue) mTorr in the collision cell. Right: Enlarged graph of C-H and C-D reaction channels.

Table S1. Calculation of KIE for C-H activation from 1,4-cyclohexadiene by **7b** (m/z 366).

Pressure [mTorr]	KIE C/D	Max intensity (H)	Max intensity (D)
0.2	2.41	0.00189	7.85E-04
0.3	2.59	0.00379	0.00147

Gas phase reactivity (**7b**, m/z 366)

Kinetic energy distribution of $[\text{Cu}(\text{TPA-nitrene})]^+$ (m/z 366) and the zero collision energy.

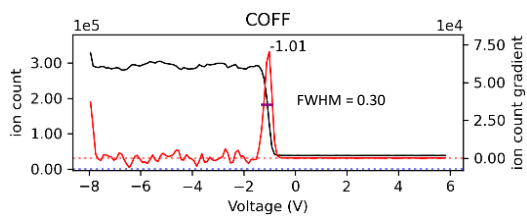


Figure S10 Kinetic energy distribution of **7b** and the zero collision energy.

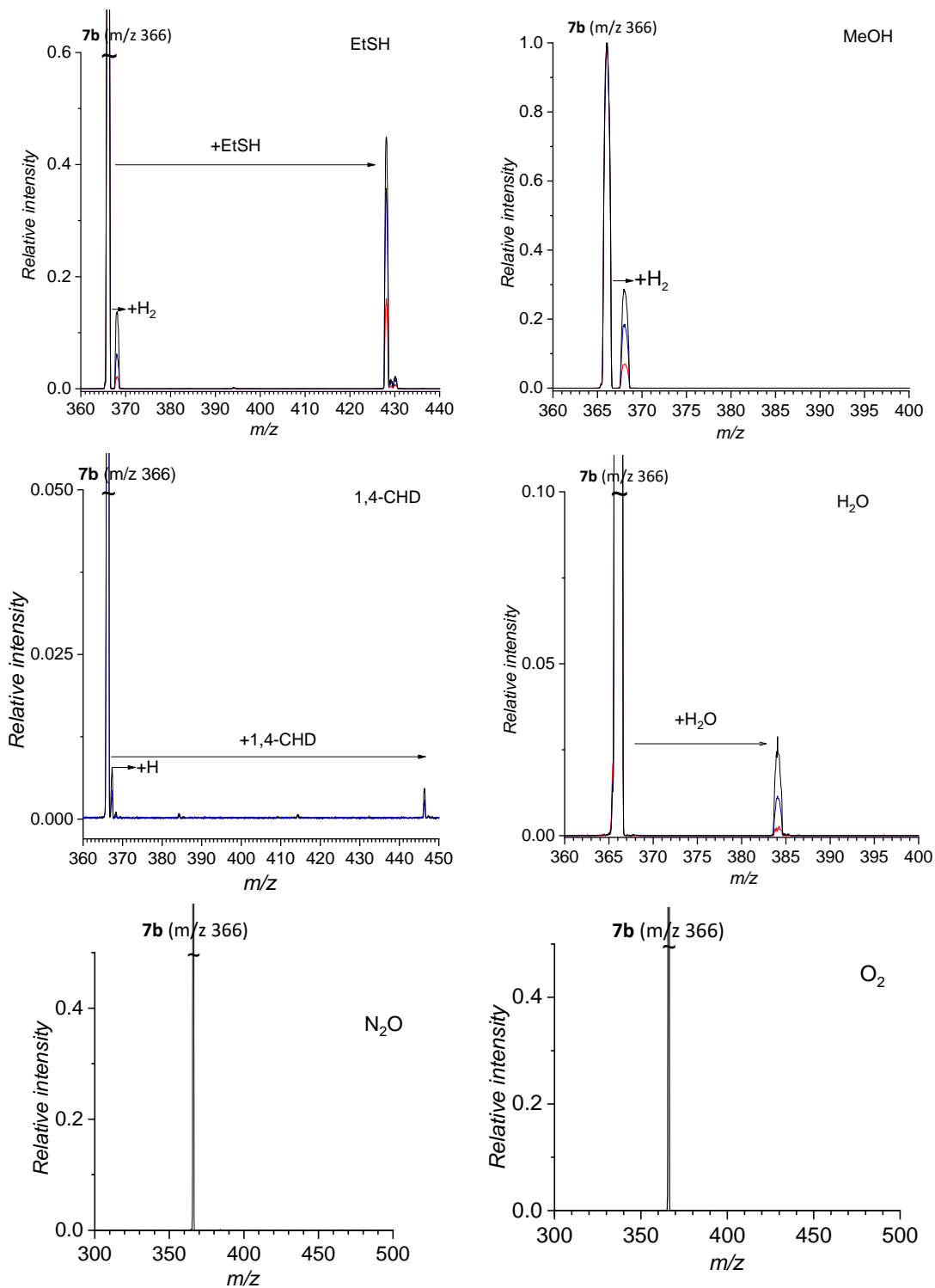


Figure S11. Gas phase reactivity of **7b** (m/z 366) at zero collision energy with ethane thiol (top left), methanol (top right), 1,4-CHD (middle left), H₂O (middle right), N₂O (bottom left) and O₂ (bottom right). Substrate pressure was 0.1 (red), 0.2 (blue) or 0.3 (black) mTorr.

[Cu(TPA-OH)]⁺

The fragment generated by in-source fragmentation of **1a** (loss of ClO₂ radical, m/z 369) (Figure S1) was characterized with helium tagging IRPD (Figure S12). Theoretical calculated spectra of [Cu(TPA-OH)]⁺ (**12a**⁺) is in good agreement with the measured spectrum. For [Cu(TPA)O]⁺ (**3a**⁺) complex the spectra does not match between 1000 and 1200 cm⁻¹ confirming ligand oxidation.

Furthermore, the generated ion (m/z 369) shows no significant reactivity towards 1,4-cyclohexadiene (Figure S13). Based on these results the generated fragment is assigned as the oxidized ligand [Cu(TPA-OH)]⁺ (**12a**⁺).

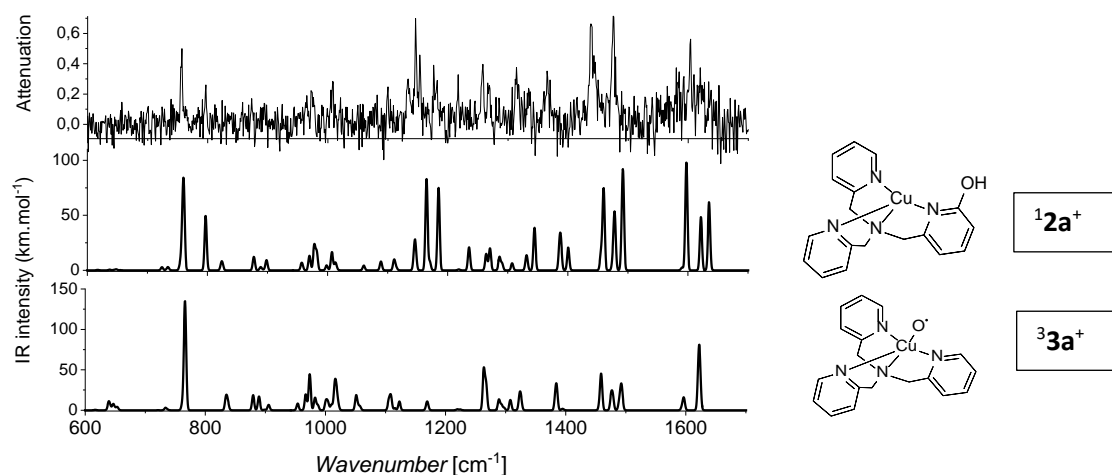


Figure S12. Top spectra is the helium tagging IRPD spectra of m/z 369. The data was smoothed. The middle and bottom IR spectra are calculated (B3LYP-6-31G+G*) and scaled by 0.97 factor to correct for anharmonicity.

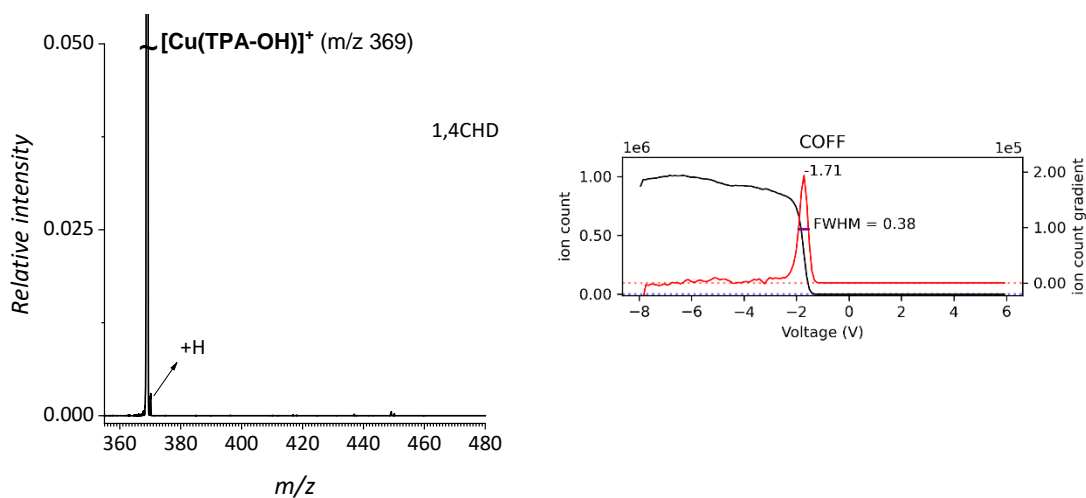


Figure S13. Left: Gas phase reactivity of **1b** with 1,4-cyclohexadiene (0.3 mTorr) at zero collision energy. Right: Kinetic energy distribution and zero collision energy of m/z 369 [Cu(TPA-OH)]⁺.

Potential energy surfaces

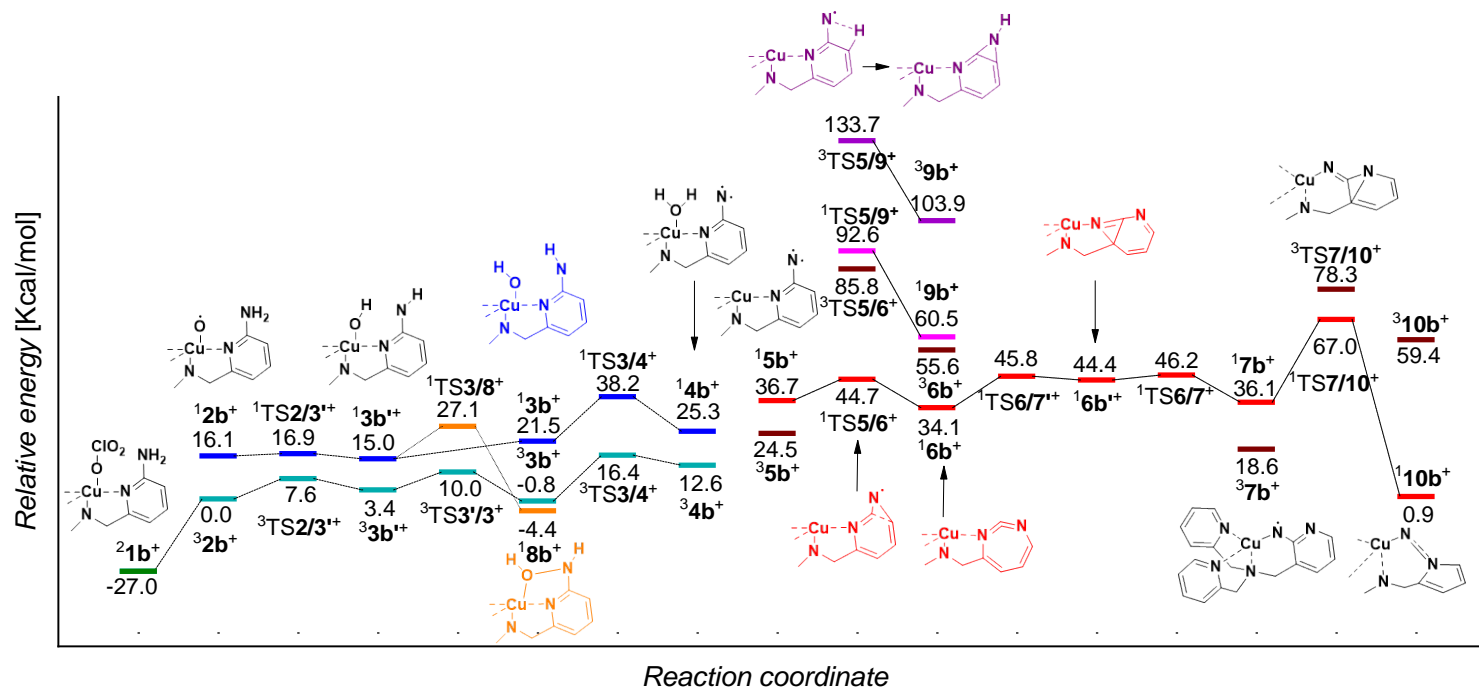


Figure S14. Potential energy surface for fragmentation and rearrangement of **1b**. Structures were calculated on B3LYP level with 6-31+G* basis set. Relative energies at 0K are presented in Kcal/mol. Most structures have a truncated representation, but all calculations were performed with the whole ligand.

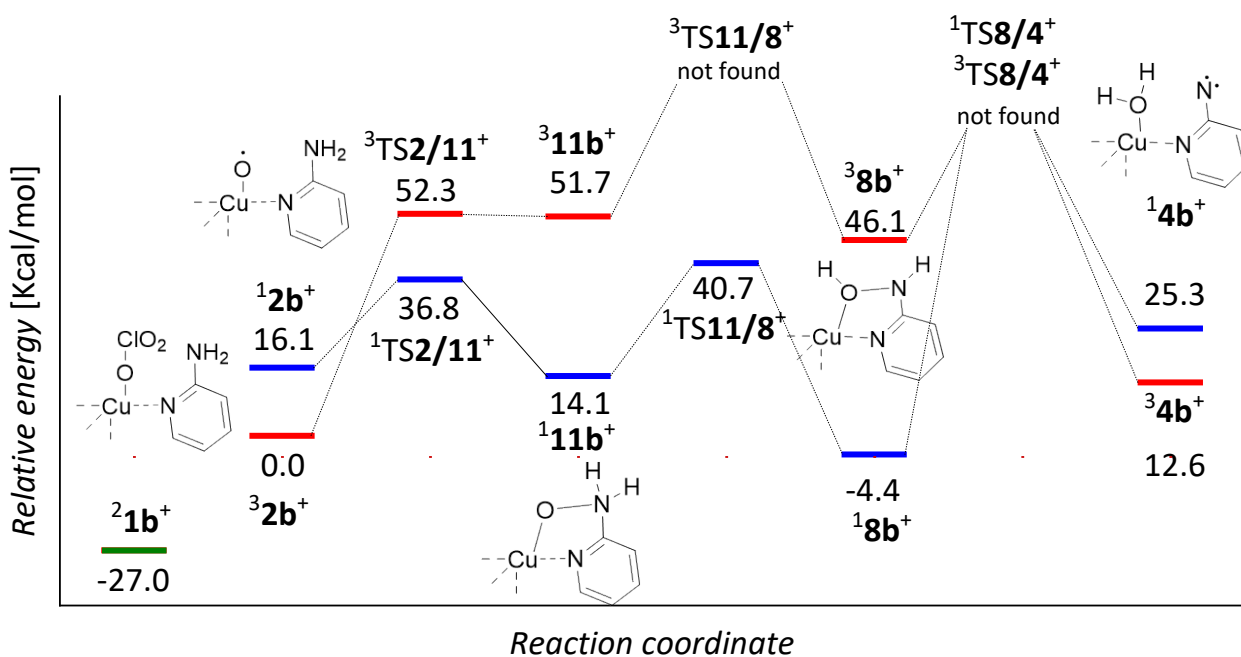


Figure S15. Potential energy surface for oxidative addition reaction after fragmentation of ClO_2 radical from $\mathbf{1b}$. Relative energies at 0 K are presented in Kcal/mol.

References

1. Gaussian 16, Revision C.01, Frisch, M. J.; Trucks, G. W.; Schlegel, H. B.; Scuseria, G. E.; Robb, M. A.; Cheeseman, J. R.; Scalmani, G.; Barone, V.; Petersson, G. A.; Nakatsuji, H.; Li, X.; Caricato, M.; Marenich, A. V.; Bloino, J.; Janesko, B. G.; Gomperts, R.; Mennucci, B.; Hratchian, H. P.; Ortiz, J. V.; Izmaylov, A. F.; Sonnenberg, J. L.; Williams-Young, D.; Ding, F.; Lipparini, F.; Egidi, F.; Goings, J.; Peng, B.; Petrone, A.; Henderson, T.; Ranasinghe, D.; Zakrzewski, V. G.; Gao, J.; Rega, N.; Zheng, G.; Liang, W.; Hada, M.; Ehara, M.; Toyota, K.; Fukuda, R.; Hasegawa, J.; Ishida, M.; Nakajima, T.; Honda, Y.; Kitao, O.; Nakai, H.; Vreven, T.; Throssell, K.; Montgomery, J. A., Jr.; Peralta, J. E.; Ogliaro, F.; Bearpark, M. J.; Heyd, J. J.; Brothers, E. N.; Kudin, K. N.; Staroverov, V. N.; Keith, T. A.; Kobayashi, R.; Normand, J.; Raghavachari, K.; Rendell, A. P.; Burant, J. C.; Iyengar, S. S.; Tomasi, J.; Cossi, M.; Millam, J. M.; Klene, M.; Adamo, C.; Cammi, R.; Ochterski, J. W.; Martin, R. L.; Morokuma, K.; Farkas, O.; Foresman, J. B.; Fox, D. J. Gaussian, Inc., Wallingford CT, 2016.
2. J. Roithová and D. Gerlich, *Int. J. Mass Spectrom.*, 2013, **355**, 204–210.
3. J. Roithová, A. Gray, E. Andris, J. Jašík and D. Gerlich, *Acc. Chem. Res.*, 2016, **49**, 223–230.